Preparation and Characterization of a Thermoplastic Poly(Glycerol Sebacate) Elastomer by Two-Step Method

Quanyong Liu,[1] Ming Tian,[1] Tao Ding,[1] Rui Shi,[1] Yuxing Feng,[1] Liqun Zhang,[1,2] Dafu Chen,[3] Wei Tian[3,4]

[1]*Key Laboratory of Beijing City on Preparation and Processing of Novel Polymer Materials, Beijing University of Chemical Technology, Beijing 100029, People's Republic of China*
[2]*Key Laboratory for Nanomaterials, Ministry of Education, Beijing 100029, People's Republic of China*
[3]*Laboratory of Bone Tissue Engineering of Beijing Research Institute of Traumatology and Orthopaedics, Beijing 100035, People's Republic of China*
[4]*Department of Spine Surgery of Beijing Jishuitan Hospital, the Fourth Clinical Medical College of Peking University, Beijing 100035, People's Republic of China*

Received 15 October 2005; accepted 4 March 2006
DOI 10.1002/app.24394
Published online in Wiley InterScience (www.interscience.wiley.com).

ABSTRACT: A thermoplastic poly(glycerol sebacate) elastomer (TMPGS), prepared by a two-step method for the first time, is characterized in the present work. First, non-crosslinked poly(glycerol sebacate) (PGS) prepolymers at the 1 : 1 molar ratio of glycerol to sebacic acid were synthesized through a condensation reaction. Second, TMPGSs were achieved through prepolymers that continued to react after the addition of more sebacic acid at a total molar ratio of 2 : 2.5 (glycerol/sebacic acid). The swelling experiments demonstrated that its crosslinking density was low and that it was composed of sol and gel. Compared with our previous results, the content of sol decreased but still reached >60%. Differential scanning calorimetry (DSC) studies demonstrated that TMPGS was crystallizable and had a glass transition temperature below −20°C, but at close to 37°C, its state altered and became almost amorphous. It was explained that both the semi-interpenetrated polymer networks composed of sol and gel and the crystal regions imparted thermoplasticity to the elastomer. Finally, the in vitro degradation tests illuminated the degradation characteristic of TMPGS in 37°C phosphate buffered saline solution (pH = 7.4). © 2006 Wiley Periodicals, Inc. J Appl Polym Sci 103: 1412–1419, 2007

Key words: elastomers; degradation; gels; thermoplastic; networks

INTRODUCTION

Biodegradable polymers[1–3] have broad application in biomedical fields, such as surgical sutures,[4,5] matrices for drug delivery, and scaffolds in tissue engineering. They play a very significant role as biomaterials.[6–10] To gain the elasticity possessed by many tissues and organs,[11–13] biodegradable elastomers, one branch of biodegradable polymers, have recently been of special interest to many investigators.[14]

Biodegradable elastomers are generally of two types: thermoplastic elastomers and thermoset elastomers. Thermoplastic elastomers are usually phase-separated block copolymers,[15–17] while thermoset elastomers are the products sometimes formed after crosslinking of the star-shaped prepolymers.[18–22] Thermoplastic elastomers are easily fabricated by melting processing; however, the crystallized hard regions possessed by these materials slow their biodegradation, and the remaining dimension is poor. In contrast, thermoset elastomers cannot be shaped by melting processing, but the speed of biodegradation is more uniform, and the remaining dimension is better. Biodegradable thermoplastic and thermoset elastomers both have their respective advantages.[23–25]

The biodegradable poly(glycerol sebacate) (PGS) elastomers were shown to have good flexibility, biocompatibility, and biodegradation in work carried out by Wang and colleagues,[24,26] PGS elastomers were also reported to be a thermoset product. Inspired by the success of Wang's group, and in an effort to explore the thermoplastic property of the elastomer, which would be very beneficial to processing of the material, we have also conducted studies of the preparation of the PGS elastomers based on glycerol and sebacic acid.[28] We have found that the product has a certain thermal-moldable ability that can be achieved at a different molar ratio, but the overall properties of the elastomer still need improvement. In the present work, a two-step preparation method is put forward as shown in Figure 1; the thermoplastic elastomer (TMPGS) is obtained in a similar manner. As a result, the gel content of TMPGS increases, strength and elongation become greater, and the in vitro degradation

Correspondence to: L. Zhang (zhanglq@mail.buct.edu.cn).
Contract grant sponsor: Key Project of Beijing National Science Foundation; contract grant number: No. 2061002.

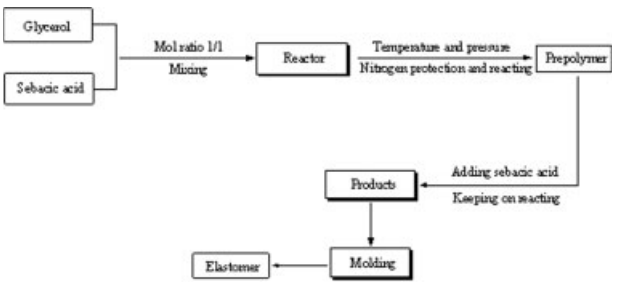

Figure 1 Method of two-step preparation of TMPGS elastomer.

rate is slower, as compared with the results obtained at the same molar ratio of reactants in our previous study.[28] Research on TMPGS elastomers prepared by the two-step method may greatly extend the development of PGS elastomers in the biomaterial fields.

EXPERIMENTAL

Materials

Glycerol (analytical grade, weight content >99.0%) was obtained from the Beijing Chemical Plant. Sebacic acid (analytical grade, weight content >99.0%) was obtained from the Guangfu Fine Chemical Institute of Tianjin. Tetrahydrofuran (analytical grade) was obtained from the Beijing Century Red-Star Chemical Limited Corporation. All reagents were used directly.

Preparation of TMPGS elastomer by two-step method

Figure 1 shows the method of preparation for TMPGS. Glycerol and sebacic acid were mixed in flask at a molar ratio of 1 : 1 and were then heated until the monomers melted completely within ~ 1 h at a pressure of 2 kPa. After controlling the condition of 130°C and 1 kPa and maintaining the reaction for some time, the prepolymers were attained. Adding a specific sebacic acid into the flask and allowing the total molar ratio to reach 2 : 2.5 (glycerol/sebacic acid), while again continuing the reaction at 130°C and 1 kPa, the desired products were achieved. Nitrogen ran slowly into the flask continuously throughout the process. The above products were taken out of the flask and hot-pressed at 130°C and 15 MPa in a window mold and were then transferred into another cold-press machine and molded at room temperature for 20 min.

Characterization of prepolymers

To investigate the structure of the prepolymer, a Bruker AV600 nuclear magnetic resonance (NMR) spectrometer (Zurich, Switzerland) was employed to determine the ^{1}H NMR spectrum, which worked at 600.13 MHz for a proton in chloroform-d_6, with tetramethylsilane as the standard. The number average molecular weight (M_n), weight average molecular weight (M_w), and polymer distribution index (PDI) of the prepolymer were reported by gel permeation chromatography (GPC) measurements on a Waters instrument equipped with three columns (Styragel HT3, HT5, and HT6E), using tetrahydrofuran as the eluent and a Waters 2410 refractive index detector. The polystyrene standard was used for calibration.

Characterization of TMPGS

The infrared (IR) spectra of the elastomer was recorded on a Nicolet-210 spectrophotometer (Madison, WI), using KBr salt flake pressed together with the fragments of elastomer film.

The sol content of the elastomer and swelling degree of the corresponding gel were measured through the following swelling tests[25]: a small disc sample (1-mm thickness and 10-mm diameter, ~ 0.09-g weight) weighing W_1 was dipped into tetrahydrofuran (20 mL) for 24 h and was then taken out. The disc was recorded with the weight of W_2 after the solvent on its surface was absorbed by filter papers; the disc was then dried to a constant weight W_3 in a vacuum oven. Sol content: $Q = (W_1 - W_3)/W_1 \times 100\%$, and the swelling degree of corresponding gel was reported as follows: $R = (W_2 - W_3)/W_3 \times 100\%$. Two samples were applied in each experiment, and the average value was adopted. To obtain the sol composition, especially the sebacic content in elastomers and the molecular weight, the sol solution in tetrahydrofuran that remained after the swelled gel was taken out and analyzed with the GPC instrument.

The thermal properties of the elastomer (composed of gel and sol) and their corresponding gel parts (obtained by dipping the elastomer in tetrahydrofuran for 24 h and then drying them to a constant weight) were evaluated with a differential scanning calorimeter (DSC; Perkin-Elmer, Norwalk, CT) test at a heating and cooling rate of 10°C/min. The sample (17–20 mg) placed in an aluminum pan was first heated from 40°C to 150°C and held there for 5 min; the cooling scan was then recorded from 150°C to −100°C; subsequently, a second heating scan was conducted from −100°C to 150°C.

The specimens for mechanical testing were cut from the 1-mm-thick samples according to ISO/DIS 37–1990 type 3 specifications (dumbbell-shaped specimens, width = 2 mm). Tensile tests were performed in a universal tensile testing machine equipped with a 50*N* load cell and operated at a cross-head speed of 50 mm/min. The elongation of the specimen was derived from an extensometer separation of 15 mm.

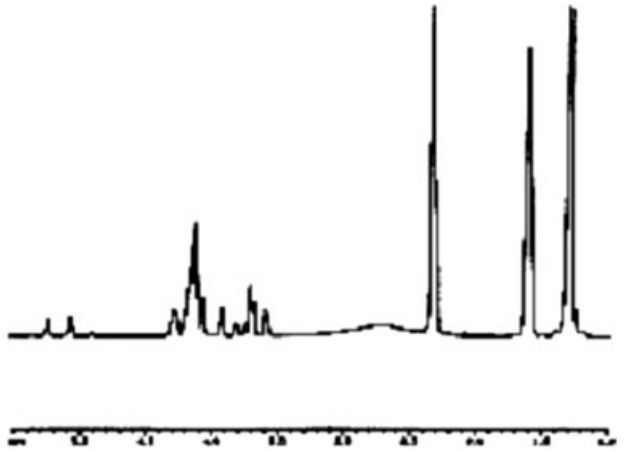

Figure 2 ^{1}H NMR spectrum of the prepolymer (chloroform-d_6 as solvent and tetramethylsilane as standard).

The Young's modulus was determined from the initial slope of the stress–strain curve (1–5% strain range of stress–strain curve). Three samples were tested at 23°C.

The equilibrium water uptake in deionized water was defined as the fraction of gained weight of a small disc sample. Water uptake: $U_1 = (M_2-M_1)/M_1 \times 100\%$, $U_2 = (M_2-M_3)/M_2 \times 100\%$, where M_1 was the initial weight of the specimen, M_2 was the weight after the specimen was dipped in deionized water for 24 h, and M_3 was the weight of the specimen first dipped in deionized water for 24 h and then dried to a constant weight in a vacuum oven. Three samples were tested, and the average value was then obtained.

The hydrophilicity of the elastomer was characterized by measuring the water-in-air contact angle of smooth surfaces of 1-mm-thick samples with the Germany Dataphysics OCA20 water contact angle measurement instrument. The sessile drop method was adopted and the result was the average of 5 values.

The small disc samples (10-mm diameter and 1-mm thickness, ~ 0.09-g weight) were used for in vitro degradation study. The authors mainly considered hydrolysis degradation. The sample weighed G_1 was placed in a taper bottle and immersed in phosphate-buffered saline (PBS, pH = 7.4) at 37°C in a oven. The PBS was replaced every 2 days to ensure a constant pH value of 7.4. The samples were removed after a planned time (1d, 4d, 6d, 13d, 20d, 27d), washed three times with deionized water, and then dried to a constant weight of G_2 in vacuum oven. The mass loss was calculated as follows: mass loss $= (G_1-G_2)/G_1 \times 100\%$. Three specimens were tested to achieve the average value. To analyze further the degradation of the elastomer, the residue elastomers experienced different degradation time were characterized again through DSC measurement, swelling tests and GPC measurements.

RESULTS AND DISCUSSION

GPC and ^{1}H NMR analysis of prepolymers

The M_n, M_w, and PDI of PGS prepolymers were 1681, 2696, and 1.60, respectively. Figure 2 shows the ^{1}H NMR spectrum of the prepolymers. The hydrogen proton peaks were classified as follows.[29–31] Some of the hydrogen proton peaks appear to be dispersive in Figure 2. For example, the chemical shift representing d hydrogen proton was within the range of 3.577–3.927 ppm. The phenomenon may be caused by the collective effect of a different molecular structure environment and hydrogen action strength in the distributive prepolymers. The hydrogen proton peak of hydroxyl groups was wide and could be distinguished with D_2O.

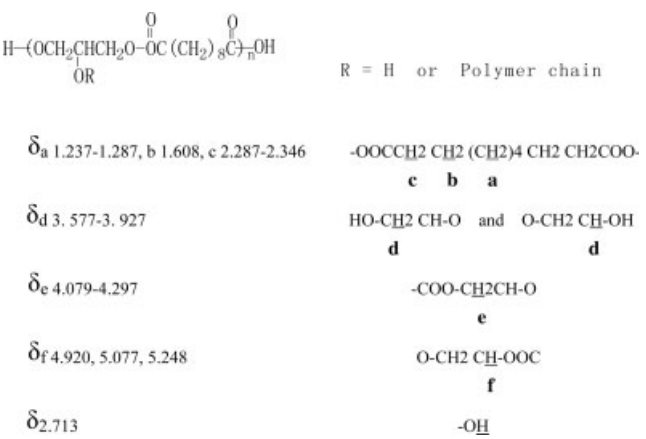

The area of different proton peaks was measured. The actual molar ratio of the reactants, the degree of esterification of different hydroxyls in glycerol, and the percentage of residue hydroxyl groups in the prepolymers were calculated according to the following formulas:

Actual molar ratio (glycerol/sebacic acid): $F = 16S\delta_{-d,e,f}/\ 5S\delta_{-a,b,c}$

Esterification degree of —CH_2—OH (1*M* glycerol): $E_1 = 5S\delta_{-e}/6S\delta_{-d,e,f}$

Esterification degree of —CH—OH (1*M* glycerol): $E_2 = 5S\delta_{-f}/3S\delta_{-d,e,f}$

Percentage of residual hydroxyl (1*M* glycerol): $N = 1-5S\delta_{-e}/6S\delta_{-d,e,f}\ -5S\delta_{-f}/3S\delta_{-d,e,f}$

S = the area of peaks; δ = chemical shift (ppm); a,b,c,d,e,f = category of hydrogen protons

The actual molar ratio of the reactants was 0.97 : 1; the esterification degree of —CH_2—OH and —CH—OH were 53.48% and 11.33% in turn; and the percentage of residual hydroxyl was 35.19%. In theory (^{1}H NMR analysis), the maximum esterification degree of —CH—OH is 33.33% (1/3) and the maximum esterification degree of —CH_2—OH is 66.67%

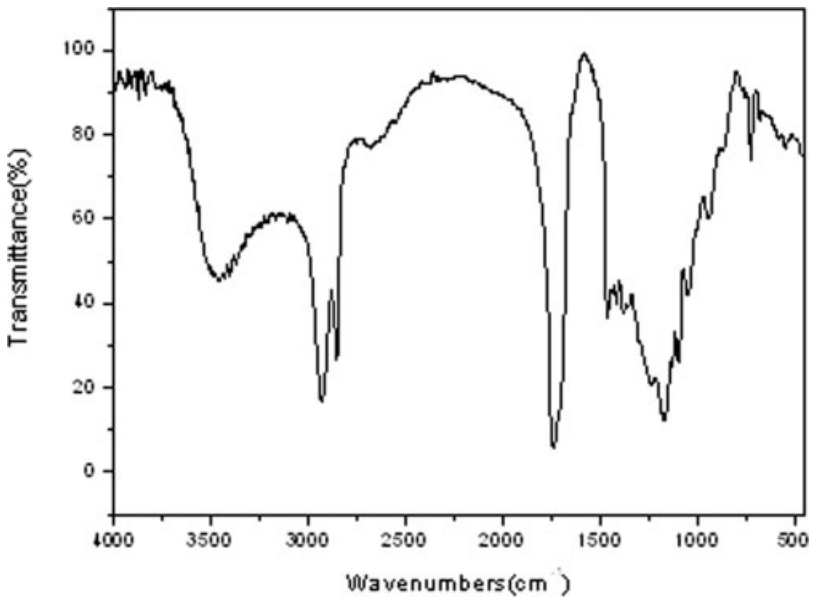

Figure 3 IR spectrum of the elastomer (KBr salt flake pressed with the fragments of elastomer film).

(2/3). But the actual results are lower, which proves that many hydroxyl groups still exist in the prepolymer as the percentage of residual hydroxyl shown. Furthermore, most residual hydroxyl groups belong to —CH—OH, which indicates that the branching degree of prepolymer is low. The presence of many hydroxyl groups provided the chance for a reaction for the prepolymers at the next step reaction.

Characterization of TMPGS elastomer

Figure 3 showed FTIR spectra of the elastomer. The absorption at 2686 cm^{-1} belonged to the hydroxyl groups in carboxyl, which proved the existence of carboxyl groups in the elastomer. The absorption at 1747 cm^{-1} belonged to the ester carbonyl, which displayed the formation of ester in reactions. The absorption at 3461 cm^{-1} was demonstrated by the hydroxyl groups that were not in the carboxyl group, at lower wavenumbers compared with that of the free hydroxyl groups. This finding demonstrated the stronger action of hydrogen bonding in the elastomer. The carboxyl and hydroxyl groups may provide the elastomer with good surface property, good biocompatibility, and functional points when the elastomer requires chemical modification.

Figure 4 shows the GPC curves of sol in the elastomer and pure sebacic acid. The GPC curve of sol displayed two distinct peaks (P_1, P_2), indicating that the sol was composed mainly of two components with different molecular weights. It appears that the small P_2 peak would grow up on the wide P_1 peak. A slight side step occurred on the leftmost position of P_2 peak, perhaps the result of the large transformation of molecular weight and branch degree of the sol. Comparison of the GPC curve of sol with that of sebacic acid indicates that the P_2 peaks of sol might correspond to sebacic acid, and P_1 might be related to the sol. Subsequently, the sebacic content of the sol could be determined to be 13.56% by GPC measurement. Some sebacic acid in the elastomer will act as a plasticizer to

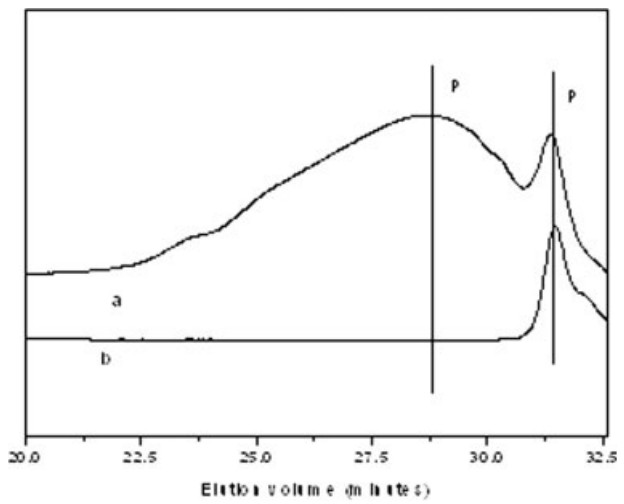

Figure 4 GPC curves of TMPGS elastomer sol. The sol solution originates from the solution remaining after the swelling experiment of the sample in 20 mL tetrahydrofuran, and ~ 0.09 g in the weight of initial disc sample. Curve a, sol; curve b, pure sebacic acid.

TABLE I
DSC Results of the Elastomer (Sol and Gel) and Gel Parts

Elastomer	T_g (°C)	T_m (°C)	T_c (°C)		−ΔH (J/g)
Sol and gel	−22.5	5.6	−14.3	23.4	61.35
Gel parts	−26.4	2.0	−18.5	—	28.37

contribute to the thermoplasticity of material. The M_n and M_w of sol were simultaneously reported as 3335 and 15,715, respectively. It could be concluded that the elastomer was a low crosslinking degree material with the swelling degree of 2112%, consisting mainly of sol with a sol content of 61.87%. However, both the sol content and swelling degree of the elastomer prepared by the two-step method became lower than at the same molar ratio of the reactants in the previous work. Thus, not only did the gel content of elastomer improve, but the crosslinking density of the corresponding gel increased as well.

Table I summarizes the glass transition temperature (T_g), melting temperature (T_m), crystallization temperature (T_c), and absolute crystallization enthalpy ($-\Delta H$) of the elastomer and the corresponding gel parts. From the data of Table I, T_g, T_m, and $-\Delta H$ of the elastomer were higher than the corresponding gel. T_c of the elastomer displayed two, while T_c of the corresponding gel showed only one. The DSC melting and crystallizing curves were investigated and are shown in Figures 5 and 6. It can be seen that the elastomer had two crystallization temperatures of $<0^\circ C$ and near room temperature, but the gel parts only had one crystallization temperature that was lower than the elastomer at a similar position. As a result, the elastomer is crystallizable, and the crystallization at $<0^\circ C$ originates mainly from the gel parts, while the crystallization near room temperature comes from the sol parts. The existence of sol parts will influence the crystallization of gel parts to a some extent. The glass transition behavior could be observed in the melting curves of both the elastomer and gel parts.

As a result of DSC measurement, the elastomer is crystallizable, and crystal regions and amorphous regions results in microphase separation structure at room temperature. The amorphous regions will impart elasticity and network structure to the elastomer, while the crystal regions will provide strength, stiffness, and thermoplasticity. Furthermore, at near 37°C, the elastomer will bring about an altered state, which makes the elastomer almost fully amorphous. The microphase separation structure at room temperature and the altered state at near 37°C will be worth concerning to find its certain application in the biomedical fields.

The tensile strength, Young's modulus, and elongation at a break of the elastomer were 0.61 ± 0.06 MPa, 0.55 ± 0.23 MPa, and 236.62 ± 31.44%. The stress–strain curve is displayed in Figure 7. The mechanical properties of elastin change within a certain range: Young's modulus, 0.3–0.6 MPa, tensile strength, 0.36–4.4 Mpa; and elongation at break, 100–220%.[31] The elastomer that was prepared had mechanical properties similar to those of elastin, which might provide a mechanical base in the biomedical application.

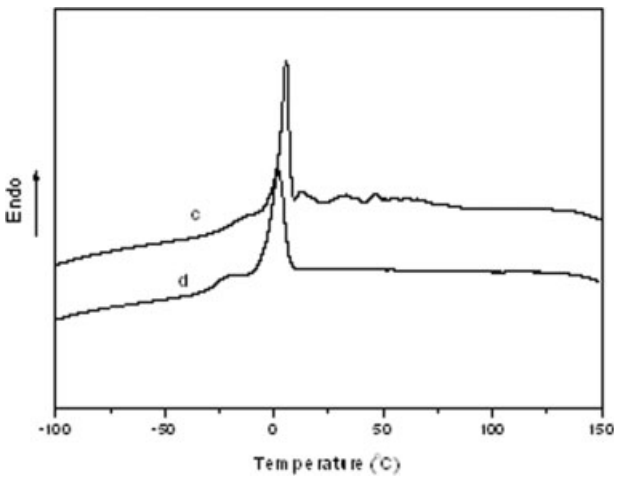

Figure 6 DSC melting curve (heating from −100°C to 150°C at rate of 10°C/min). Curve c, elastomer; curve d, gel part of elastomer.

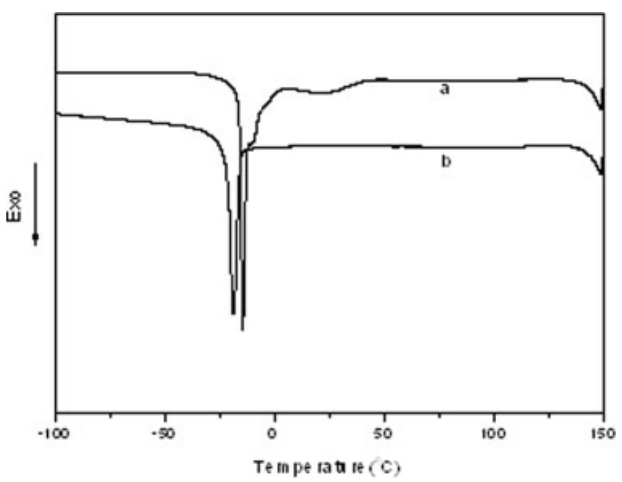

Figure 5 DSC crystallization curve (cooling from 150°C to −100°C at rate of 10°C/min). Curve a, elastomer; curve b, gel part of elastomer.

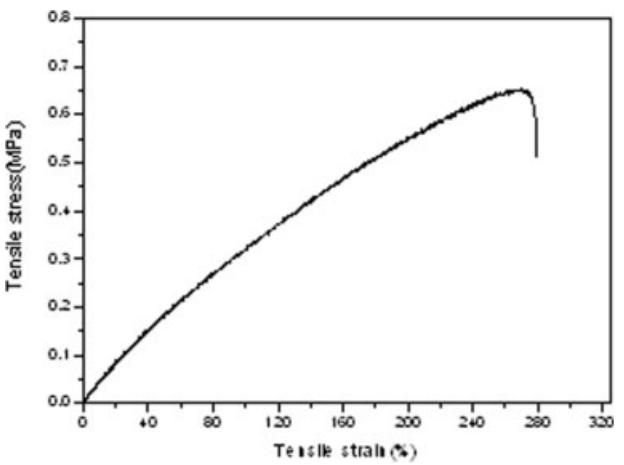

Figure 7 Stress–strain curve of the elastomer (dumbbell-shaped specimens, thickness = 1 mm, width = 2 mm; 50*N* load cell and cross-head speed of 50 mm/min).

The elastomer could absorb some water to extent, which would be advantageous to its biodegradability. The value of U_1 was 8.24%, and U_2 was 11.67%. The difference between U_1 and U_2 showed the elastomer had been degraded partly in the course of the water-absorbing testing. So, combining the results of U_1 and U_2 will provide a good description of the water-uptake property of the elastomer.

The hydrophilicity of a material is a property that controls protein deposition, cell affinity, and degradation rate. The water-in-air contact angle of the elastomer was 37.8° that demonstrated it had the good hydrophilicity.

Figure 8 shows the mass loss-time curve of the elastomer in 37°C PBS, at pH 7.4, at different degradation periods (1, 4, 6, 13, 20, and 27 days), which characterized the in vitro degradation. The mass loss of the elastomer was ~ 15% after 1-day degradation; the mass loss rate then decreased at other periods. Here, it can be speculated that sol in the elastomers will degrade out in preference to gel because of the crosslinked network structure of the gel, and the possibility of the sol degrading out of the elastomer will relate to its molecular weight and hydrogen bonding with other molecules.

To carry out an in-depth investigation of the structure and composition change of the elastomer during degradation, they were characterized by DSC, swelling tests, and GPC test, respectively, at different degradation periods.

Table II summarizes the results of DSC measurement on the elastomer undergoing degradation at the different periods (0, 1, 6, and 20 days). The data presented in Table II, T_g, T_m, and $-\Delta H$ of the elastomer show a tendency to decrease with increased degradation time. Clearly, T_g, T_m, T_c, and $-\Delta H$ of the elastomer all altered primarily after 1-day degradation. For example, the elastomer exhibited only one crystallization temperature after 1-day degradation, which was different from that (two temperatures) before degradation and close to that of the elastomer at lower temperature crystallization, corresponding to the gel structure. But at the latter periods, all the data were close.

TABLE II
DSC Results of the Elastomer Undergoing Different Time Degradation

Day	T_g (°C)	T_m (°C)	T_c (°C)		$-\Delta H$ (J/g)
0	−22.5	5.6	−14.3	23.4	61.35
1	−25.1	3.6	−17.9	—	25.85
6	−25.9	3.7	−18.4	—	24.88
20	−26.1	2.8	−18.5	—	24.48

To explain this phenomenon, Figure 9 shows the GPC curve of the residual elastomer of the sol after 1-day degradation. The curve in Figure 9 displays only one wide peak. Compared with the GPC curve of sebacic acid, the small peak represents the disappearance of sebacic acid. It was clearly found that sebacic acid in the elastomer hardly existed after only 1-day degradation. Here, combining the results of Figure 8, Table II, and Figure 9, it can be inferred that the mass-loss (~ 15%) of the elastomers during day 1 of degradation is attributable mainly to the dissolving out of all the sebacic acid (~ 10%) and the degradation of some of the sol (~ 5%) in the elastomers. In the latter period, the slow degradation of the elastomer is caused by common degradation of gel part and sol part; however, the sol part preferentially degrades out.

Figure 10 displays the swelling degree and sol content of the residue elastomer after different time degradations. The sol content of the elastomer first increased slightly during day 1 degradation and then decreased distinctly from day 1 to the day 6, and then

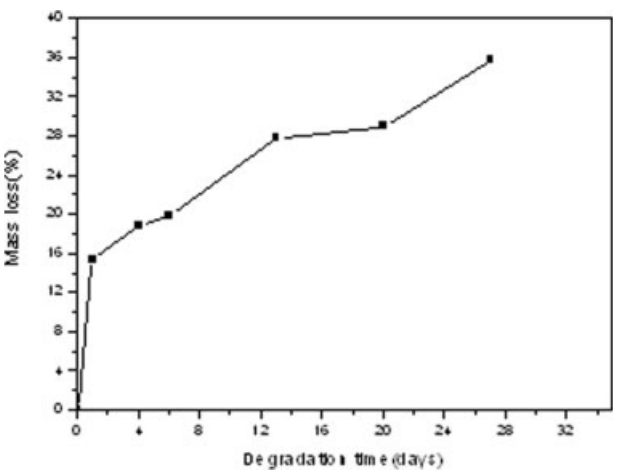

Figure 8 Mass loss-time curve of the elastomer (disc samples of 10-mm-diameter and 1-mm thickness, phosphate-buffered saline solution, pH = 7.4, replacing solution every 2 days).

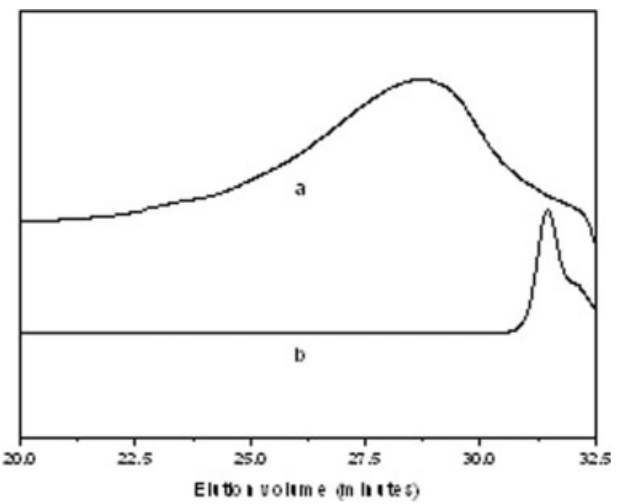

Figure 9 GPC curves of sol of the elastomer after 1-day degradation (solvent: 20 mL tetrahydrofuran). Curve a, sol; curve b, sebacic acid.

increased slightly from day 6 to day 13, finally increasing dramatically from day 13 to day 20. Combining the mass-loss time curves shown in Figure 8, this can be explained as follows: during the first day, only the low-molecular-weight sol and sebacic acid are dissolved out or degraded out of the elastomer, but the new sol part produced by gel during day 1 degradation compensates for the loss, leading to a slight increase of sol in the elastomer. After day 1, since the degradation rate of sol is higher than that of gel, in the latter period, the sol quickly degrades to the lower molecular weight and is then dissolved out of the elastomer, which exceeds the generation rate of sol from gel and leads to a decreased sol content in the elastomer. During day 6–13, the leak rate of sol from the elastomer and the generation rate of the new sol from gel approach a balance. After day 13, more and more crosslinking bonds are broken and more and more gel turns into sol molecules, resulting in a rapid increase in the sol content.

The crosslinking density of gel first decreased during the day 1 of degradation and reached the minimum on day 4, then increasing from day 4 to day 6 and reaching the maximum on day 6. The crosslinking density decreased only slightly from day 6 to day 13 and finally decreased dramatically from day 13 to day 20. It is hard to understand why the crosslinking density of elastomer increases after 6 days of degradation. The gels appear to be composed of networks with different crosslinking density. The gels with the low crosslinking density degrade to the lower crosslinking density and cause the whole crosslinking density of gel to decrease from day 0 to day 4. The gels with the lower crosslinking density then degrade to the sols and are dissolved out of the elastomer. As a result, the gels with high crosslinking density remain, demonstrating a rise in the crosslinking density of gel on day 6. After 6-day degradation, the gel appears to possess high, homogeneous crosslinking density and degrades much more slowly, which causes the crosslinking density to decrease slightly from day 6 to day 13. After day 13, with the breakup of the crosslinking bonds, the network becomes looser and looser, making the degradation quicker and quicker.

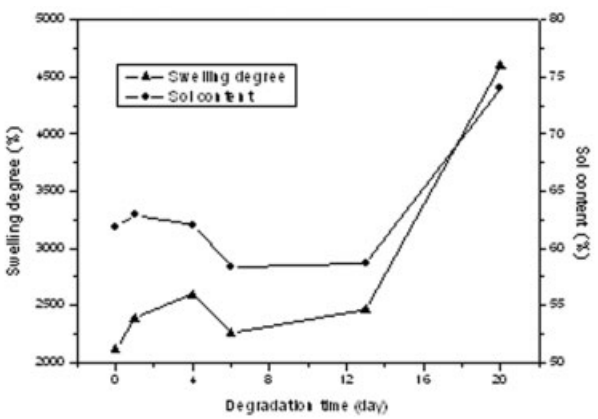

Figure 10 Swelling degree and sol content of the residue elastomer after different time degradation (to gain swelling degree and sol content, samples were dipped in 20 mL tetrahydrofuran for 24 h).

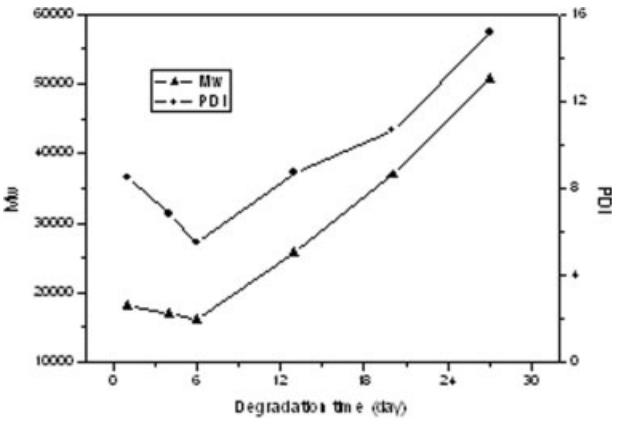

Figure 11 M_w and PDI of sol in the residue elastomer after different time degradation (the sol solution originates from the solution remaining after the swelling experiment of the samples in 20 mL tetrahydrofuran).

Figure 11 shows the M_w and PDI of sol in the residue elastomer after different time degradations. The two curves illustrate a similar trend, with M_w and PDI of sol first decreasing and then increasing during the degradation. This transition can be explained as follows. Because the sol degrades at a higher rate than the gel, at the beginning the degradation of the original sol part is mainly responsible for the decrease in the average M_w of sol in the elastomer. However, in the latter period, the gel degradation begins and breaks into new sol parts of high molecular weight, leading correspondingly to an increase of sol M_w in the elastomer. Moreover, with the degradation, the molecular weight of new sol from gel is larger and larger. As for the PDI, as the high-molecular-weight sol tends to turn into molecules of lower and lower molecular weight, the molecules of lower molecular weight tend to degrade at a relatively slow rate, because of the lower amount of degradable ester bonds in molecule chains; the result is both an decrease in average molecular weight and a decrease in PDI at the early degradation stage. In the latter period, due to the production of molecules with much higher molecular weight from degradation of gel, the molecule weight distribution of sol becomes wider and wider.

Furthermore, considering that the mass loss of the elastomer is only $\sim$ 35% after 27-day degradation, it can be speculated that the interaction between the sols, and between sol and gel mainly through hydrogen bonding, was so strong that it was difficult for the sol to degrade quickly out of the elastomer in

37°C PBS, at pH = 7.4. The degradation characteristic of the elastomer may be potentially significant in the controllable drug delivery field.

CONCLUSIONS

A TMPGS elastomer composed of sol and gel was prepared by a two-step method. It is found that the right high sol, low crosslinking density of semi-interpenetrated polymer networks and crystallization composition impart thermoplasticity to the elastomer. The overall properties of the elastomer by the two-step method are better than those previously reported by the same investigators. Some sebacic acid remains in the elastomer, possibly contributing to the initial mechanical property and processing ability of the elastomer; moreover, the sebacic acid will be degraded out of the elastomers after 1-day degradation. The elastomers exhibit their own degradation characteristic in 37°C PBS, at pH = 7.4. Thus, sol in the elastomers will be degraded out in preference to gel; the loss of elastomers of the low-weight sol relates partly to the interaction among molecules, such as hydrogen bonding.

References

1. Fisher, J. P.; Timmer, M. D.; Holland, T. A.; Dean, D.; Engel, P. S.; Mikos, A. G. Biomacromolecules 2003, 4, 1335.
2. Lwasaki, Y.; Nakagawa, C.; Ohtomi, M.; Lshihara, K.; Akiyoshi, K. Biomacromolecules 2004, 5, 1110.
3. Chen, Y.; Wombacher, R.; Wendorff, J. H.; Visiager, J.; Smith, P.; Greiner, A. Biomacromolecules 2003, 4, 974–980, .
4. Frazza, E. J.; Schmitt E. E. J Biomed Mater Res Symp 1971, 1, 43.
5. Storck, M.; Orend, K. H.; Schmitzrixen, T. Vasc Surg 1993, 27, 413.
6. Dahiyat, B. I.; Posadas, E. M.; Hirosue, S.; Hostin, E.; Leong, K. W. Reactive Polym 1995, 25, 101.
7. Kazuhiko, H.; Mie, S.; Takayuki, S.; Yoshiki, I. J Appl Polym Sci 2004, 92, 3492.
8. Liu, Y.; Guo, L. K.; Huang, L.; Deng, X. M. J Appl Polym Sci 2003, 90, 3150.
9. Engelmayr, G. C.; Hildebrand, D. K.; Sutherland, F. W. H. Biomaterials 2003, 24, 2523.
10. Calandrelli, L.; Immirzi, B.; Malinconico, M.; Volpe, M. G.; Oliva, A.; Della Ragione, F. Polymer 2000, 41, 8027.
11. Lee, S.-D.; Hsiue, G.-H.; Chang, P. C.-T.; Kao, C. Biomaterials 1996, 17, 1599.
12. Lee, S.-D.; Hsiue, G.-H.; Kao, C.; Chang, P. C.-T. Biomaterials 1996, 17, 587.
13. Yang, J.; Webb, A. R.; Ameer, G. A. Adv Mater 2004, 16, 511.
14. Amsden, B.; Wang, S.; Wyss, U. Biomacromolecules 2004, 5, 1399.
15. Deschamps, A. A.; Grijpma, D. W.; Feijen, J. J Biomater Sci Polym Ed 2002, 12, 1337.
16. Deschamps, A. A.; Grijpma, D. W.; Feijen, J. J. Polymer 2001, 42, 9335.
17. Fakirov, S.; Goranov, K.; Bosvelieva, E.; Du Chesne, A. Makromol Chem 1992, 193, 2391.
18. Graessley, W. W.; Roovers, J. Macromolecules 1979, 12, 959.
19. Lang, M. D.; Wong, R. P.; Chu, C. C. J Polym Sci Part A: Polym Chem 2002, 40, 1127.
20. Michael, A.; Carnahan, M. A.; Grinstaff M. W. J Am Chem Soc 2001, 123, 2905.
21. Minoru, N.; Tetsuya, M.; Wataru. S.; Naoto, T. J Polym Sci 1999, 37, 2005.
22. Robson, F.; Storey, S. C.; Warren, C. J. A.; Puckett, A. D. Polymer 1997, 26, 6295.
23. Kylma, J.; Seppala, J. Macromolecules 1997, 30, 2876.
24. Wang, T.; Ameer, G. A.; Sheppard, B. J.; Langer R. Nat Biotechnol 2002, 20, 602.
25. Storey, R. F.; Hickey, T. P. Polymer 1994, 35, 830.
26. Wang, Y. D.; Yu, M. K.; Langer R. J Biomed Mater Res 2003, 66A, 192.
27. Sundback, C. A.; Shyu, J. Y.; Wang, Y.; Faquin, W. C.; Langer, R. S.; Vacanti, J. P.; Hadlock, T. A. Biomaterials 2005, 6, 5454.
28. Liu, Q.; Tian, M.; Ding, T.; Shi, R.; Zhang, L. J Appl Polym Sci 2005, 28, 2033.
29. Nuria, G.; Julio, G.; Evaristo, R. Macromol Chem Phys 2002, 203, 2225.
30. Steffen, M.; Alexander, S.; Holger, F.; Rolf, M. Macromol Rapid Commun 2000, 21, 226.
31. Puskas, J. E.; Chen, Y. Biomacromolecules 2004, 5, 1141.